THE PENNSYLVANIA STATE UNIVERSITY
SCHREYER HONORS COLLEGE

DEPARTMENT OF ENGINEERING SCIENCE AND MECHANICS

SIMULATION OF HYDROCEPHALUS BASED ON MATHEMATICAL MODELING AND TECHNOLOGICAL ADVANCEMENTS

JUSTIN A. KAUFFMAN

Spring 2012

A thesis
submitted in partial fulfillment
of the requirements
for baccalaureate degrees
in Engineering Science and Mathematics
with honors in Engineering Science

Reviewed and approved* by the following:

Corina Drapaca
Assistant Professor of Engineering Science and Mechanics
Thesis Supervisor

Samia Suliman
Assistant Professor of Engineering Science and Mechanics
Honors Adviser

Judith A. Todd
P. B. Breneman Deparment Head Chair
Professor of Engineering Science and Mechanics

* Signatures are on file in the Schreyer Honors College and Engineering Science and Mechanics Office.

ABSTRACT

Hydrocephalus is a brain disease characterized by abnormalities in the cerebrospinal fluid circulation, resulting in ventricular dilation and brain's compression. Today's treatments display no statistically significant difference in their efficacy. Predictive models of brain mechanics can improve therapies. In this thesis we revisit two classic biomechanical models of hydrocephalus by Hakim and Marmarou and present corresponding numerical simulations in a simplified cylindrical geometry for the brain.

TABLE OF CONTENTS

LIST OF FIGURES

LIST OF TABLES

ACKNOWLEDGEMENTS

I would like to thank my thesis advisor Dr. Cornia Drapaca for unwavering support; for if it were not for you I would not have been able to be successful in this project. I would also like to thank my parents (Chuck and Diane Kauffman) for supporting me throughout my academic career; sometimes all you need is a little encouragement. Also I would to extend a thank you to my girlfriend Danielle Smith, for pushing me when I had a lack of motivation.

And to the Engineering Science and Mechanics Department at The Pennsylvania State University, I really need to say a special thanks to you for allowing me to have such a great academic career through exceptional guidance. I never once felt that I could not go to a professor for help and that is a great feeling. Finally to anyone who had helped me in any way with this thesis I really appreciate the help, the support, and the advice that you had given me.

Chapter 1

Introduction

Hydrocephalus is a serious neurological disorder characterized by excessive accumulation of cerebrospinal fluid (CSF) in the ventricles of the brain, resulting in ventricular dilation (Fig.1). It is usually associated with an increase in intracranial pressure. Although hydrocephalus is one of the most common disorders treated by neurosurgeons, the overall incidence and prevalence of hydrocephalus is difficult to estimate, as it can occur as an isolated entity or in association with other neurological disorders such as spina bifida, traumatic brain injury, stroke, intracranial hemorrhage, or infections of the central nervous system. In infant hydrocephalus the intracranial pressure is raised, and, as the CSF accumulates in the ventricles, the brain tissue compresses, and the ventricles and the skull expand. The most common cause of infantile hydrocephalus in the U.S. is hemorrhage in the neonatal period, particularly in premature infants. With about four million births occurring annually in the U.S., it is estimated that 20%-74% of the approximately 50,000 very-low-birth-weight infants born yearly will develop posthemorrhagic hydrocephalus [1]. On the other hand, in Sub-Saharan Africa which has one of the world's greatest disease burdens of bacterial meningitis, post-infectious hydrocephalus is the most common form of infantile hydrocephalus with more than 100,000 cases arising every year [2].

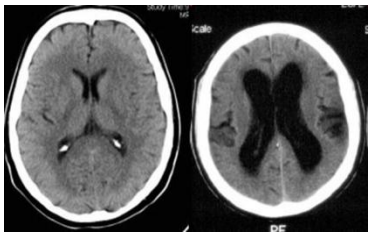

Figure 1: CT images of a normal brain (left, Neurosun website) and a brain with NPH (right, Imaging Decisions website). Note the enlarged ventricles and severely compressed brain tissue in the hydrocephalic brain

The treatment is based on CSF flow diversion. Within limits, the dilation of the ventricles can be reversed by either CSF shunt implantation or by performing an endoscopic third ventriculostomy (ETV) surgery, resulting in a relief from the symptoms of hydrocephalus. However the two treatment options display no statistically significant difference in the efficacy for treating hydrocephalus [3]. ETV works well only in appropriately selected clinical cases of hydrocephalus, whereas shunt failure occurs in over 60% of patients (Hydrocephalus statistics website). Considering that many shunt recipients are children, and that shunts are lifelong commitments, these statistics underscore the importance of improving therapy. Furthermore, the postoperative persistence of the ventricular dilation constitutes a diagnostic limit for verifying the adequate functioning of ETV in comparison with the treatment based on the placement of CSF shunt devices ([4]; see Fig.2). Therefore, knowledge of the mechanisms of ventricular dilatation during the development of hydrocephalus and of ventricular shrinkage after treatment and how these processes affect the proper functionality of the brain will help neurosurgeons determine which of the two treatments will have a better outcome. To increase the understanding of the pathophysiology of infant hydrocephalus, there is a need to design experimental and theoretical models that better explain the fundamental science behind this clinical condition.

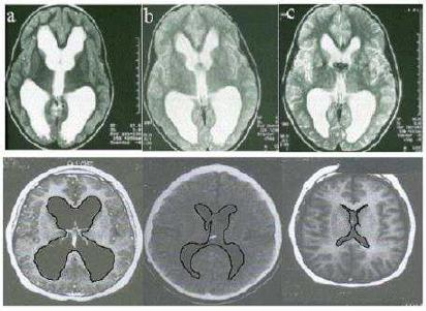

Figure 2: The first row shows MR images of a hydrocephalic brain (a) treated by ETV. The ventricular size decreased very slowly, as proved by MRI control studies 6 months (b) and 1 year (c) postoperatively [5]. The second row shows CT images of a hydrocephalic brain (a) treated by CSF shunting. The ventricular size decreased fast, as proved by CT images taken after 1 month (b) and 1 year (c) postoperatively [6].

Marmarou et al. [7] and *Hakim et al*. [8] are considered the first experimental and theoretical models of hydrocephalus. While Marmarou models the CSF dynamics and validates his model with experiments performed on cats, Hakim assumes that the brain is a viscoelastic material and proposes the first engineering approach to hydrocephalus by using a set of controlled experiments to explain the onset of hydrocephalus. In this thesis these two classic models will be revisited and also it will also be assumed that the brain tissue is a linear elastic, isotropic, homogeneous solid filling a hollow cylinder. The interior of the cylinder is filled with the CSF whose dynamics is described by Marmarou's model. We will use numerical simulations to investigate the changes in time of brain's displacements due to the dynamics of CSF described by Marmarou in [7].

The thesis is structured as follows. In chapter 2 there will be a brief review of Marmarou and Hakim's models. In chapter 3 the stress-strain analysis in a cylindrical domain using concepts from continuum mechanics, and the corresponding numerical results are shown in chapter 4. The thesis ends with a chapter of conclusions and further work.

Chapter 2

Brief Literature Review

2.1 Hakim Model

Hakim et al. [8] have provided the first engineering approach to how hydrocephalus. They proposed a mathematical framework for the study of brain's biomechanics as well as simplistic engineering systems and experiments that explained the onset of hydrocephalus from a purely mechanics point of view.

The work presented in [8] is based on years of medical evidence on the CSF dynamics. The CSF is produced by the choroid plexus located on the walls of the ventricular system and under normal conditions the CSF production has a constant rate. With age the CSF production decreases, and this is an observation that has to be considered when looking at patients with hydrocephalus. However, it is not exactly known what the rate of CSF production is and there are no realistic and robust methods and technologies to measure or estimate it [9].

The flow of the CSF starts in the lateral and third ventricles, passes through the aqueduct of Sylvius to reach the fourth ventricle. Once the CSF gets through the fourth ventricle it circulates to the subarachnoid space [9]. A portion of the CSF flows down into the lumbar subarachnoid space, which is believed to be the cause of pulsations [10]. The CSF is then absorbed by the arachnoid villi situated around the sagittal sinus [9]. It is not possible to undue absorption because the intracranial pressure (ICP) is greater than the sagittal sinus pressure (P_{ss}). Another possibility for CSF drainage is that some of the CSF can soak through into the parenchyma.

The most common cause of hydrocephalus is an obstruction in the CSF flow. For example when there is a blockage between the third and fourth ventricles the so-called non-

communicating hydrocephalus is developed and causes swelling of the lateral and third ventricles due to excess CSF accumulation [9]. This type of hydrocephalus is commonly treated with endoscopic third ventriculostomy (ETV), in which the third ventricle is punctured and the excess of CSF is allowed to drain in the brain. On the other hand communicating hydrocephalus is treated with shunts, which drain the fluid through a tube into the patient's stomach.

In [8], *Hakim et al.* describe the brain as being suspended in CSF and fixed into place from arachnoidal strands which connect the brain matter to the arachnoid membrane. The CSF is not compressing the brain but instead providing hydrostatic forces that act as a support to allow it to oppose deformation. The brain parenchyma is seen to be like a submicroscopic sponge of visco-elastic material. They observed that the brain is incompressible as a whole but the cells and cavities provide the ability for elastic deformations. This engineering point of view on the brain revolutionized this field of medicine since it contributed to the development of the shunts and hydrocephalus was finally a treatable disease.

In their seminal work [8], *Hakim et al.* also proposed two simple mechanical models, a rectilinear model, which was used to understand the CSF dynamics without considering the geometry of the brain, and a spherical model which much closely resembles the anatomical geometry of the brain. The rectilinear model (Fig.3) describes how an open venous system would interact with a closed CSF system [8]. This system looks at a small piece of the parenchymal sponge and establishes a relationship between the CSF and venous pressures. The model predicts that if the venous pressure is increased then the CSF pressure is also increased which causes a hydrostatically

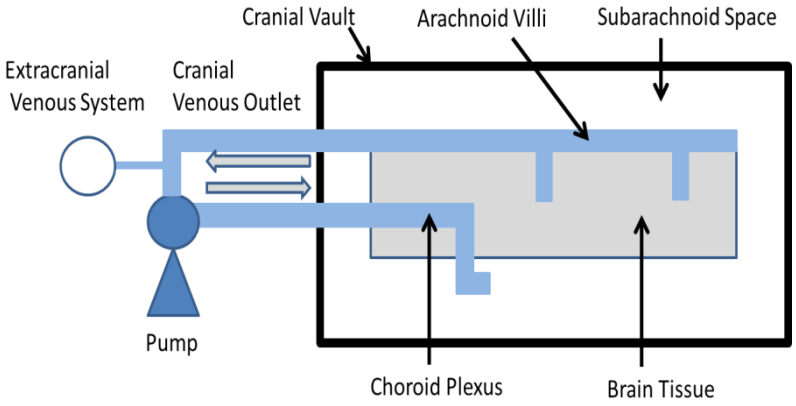

Figure 3: The Rectilinear Model.

uniform distribution of pressure around the surface of the cranial cavity. This pressure which is distributed hydrostatically does not allow the sponge to undergo deformation or to lose any of the CSF that is being retained by the cells. As long as blood is allowed to flow normally there is no tissue damage in this case. On the other hand if the CSF pressure is increased then there no longer a hydrostatic load on the brain so the brain can undergo deformations which causes the CSF to collect in the ventricular system. In addition, the loss of fluid in the brain leads to a reduction of the parenchyma's volume. This non-hydrostatic loading can cause tissue damages and is considered to model hydrocephalus.

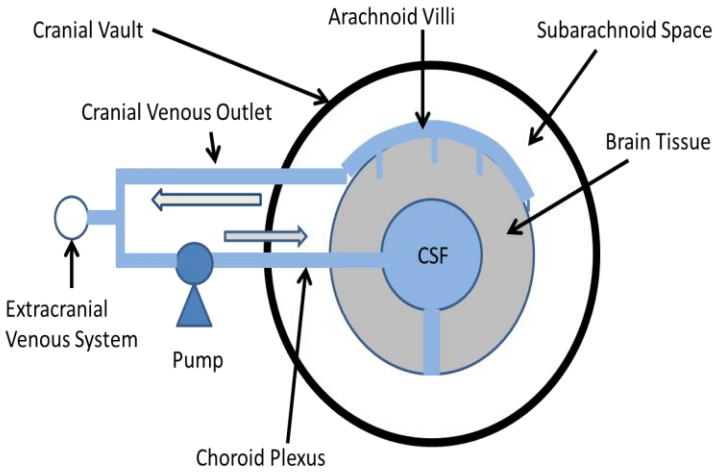

Figure 4: The Spherical Model.

The spherical model (Fig.4) has the same mechanics as the rectilinear model and also uses a three dimensional spherical geometry which is more suitable for brain's modeling. This model can provide an adequate understanding of the stress and strain distributions present in the brain during the development of hydrocephalus.

2.2 Marmarou Model

In [7], *Marmarou et al.* developed a first model for CSF dynamics that provided some essential insights into the role of ICP to hydrocephalus. In order to avoid some controversies with some terminology used in [7] that have been pointed out in the literature in the recent years, there will be no discussion here of some of the physical interpretations of Marmarou's model. The parameters that this model uses are the dural sinus pressure, the

resistance to CSF absorption and the CSF formation rate. It is important to mention that Marmarou's model has been tested on adult hydrocephalic cats and a good agreement has been established between the proposed mathematical model and the measurements [7].

They noticed experimentally that as the fluid was either added or removed from the CSF space, the pressure changed transiently and was followed by a gradual decline back down to the initial pressure. This occurs because the CSF volume and pressure are coupled. The rate of CSF formation (I_f) is composed of stored fluid (I_s) and absorbed fluid (I_a); under normal conditions the formation of fluid and the absorption of fluid balance each other so that there is no change in the amount of fluid stored. From this relationship *Marmarou et al.* developed a mathematical model that relates pressure (P) and time (t) through a nonlinear differential equation of the form:

$$\frac{dP}{dt} - \frac{P^2 K}{R} - PK\left(I_f + \frac{P_d}{R}\right) = 0 \tag{2.1}$$

where K is a constant that describes the steepness of the pressure – volume curve, R is the fluid resistance, and P_d is the intradural sinus pressure. Equation (2.1) has a solution of the form:

$$P(t) = \frac{\psi(t)}{\frac{1}{P_o} + \frac{K}{R}\int_0^\tau \psi(\tau)d\tau}, \psi(t) = e^{K\int_0^\tau I(\tau)d\tau} \tag{2.2}$$

Marmarou et al. investigated three cases that can cause a change in the CSF volume: 1) a bolus injection, 2) volume removal, and 3) continuous infusion. For each case *I(t)* is different and thus different results for *P(t)* are obtained. The analytic solutions and *I(t)* for each case are presented in Table 1. The derivation of these solutions is given in Appendix A.

Table 1: Analytic solutions of equation (2.2) for the three different cases presented in [7]. Note that P_t is the threshold pressure.

Case	*I(t)*	Analytic Solution
Bolus Injection	$I(t) = I_f + V\delta(t)$	$P(t) = \frac{P_o e^{KV+Kt(P_o/R)}}{1 + e^{KV}[e^{Kt(P_o/R)} - 1]}$
Volume Removal	$I(t) = I_f - V\delta(t)$	$\begin{cases} P(t) = P_o e^{K[I_f t - V]}, \ \ if\ P(t) < P_t \\ P(t) = \frac{P_o e^{Kt(P_o/R) - KV}}{1 + e^{-KV}[e^{Kt(P_o/R)} - 1]} \end{cases}$
Continuous Infusion	$I(t) = I_f + \Delta I$	$P(t) = \frac{P_o(P_o + R\Delta I)}{P_o + R\Delta I e^{-Kt(P_o + R\Delta I)/R}}$

Figs. 5-7 are plots of the analytic solutions to equation (2.2) corresponding to the three cases. In the bolus injection case (Fig.5) some fluid is inserted into the CSF system which adds to the formation rate of CSF. The system was in equilibrium before the fluid was added and was at an initial pressure P_o. The continuous infusion case (Fig.6) is very similar to the bolus injection case but here the ICP increases rapidly and then stabilizes.

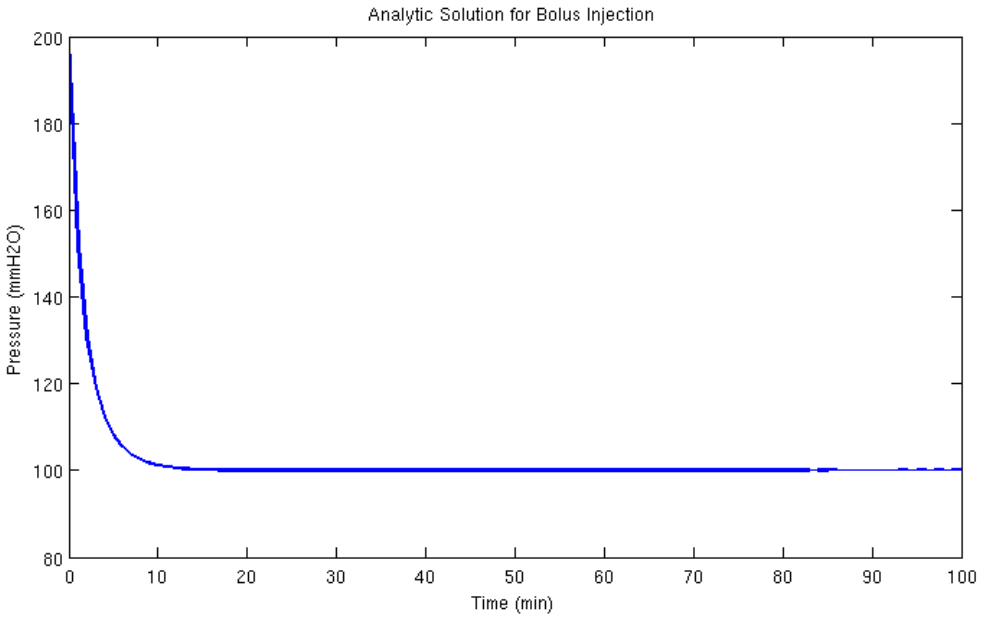

Figure 5: Analytic solution of equation (2.2) for the bolus injection case.

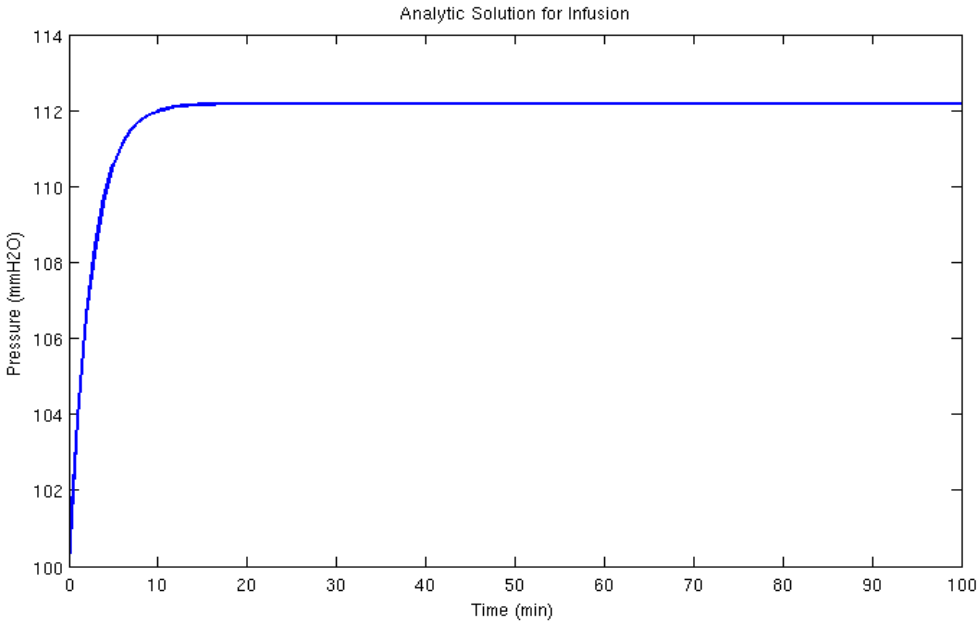

Figure 6: Analytic solution of equation (2.2) for the continuous infusion case.

In the case of volume removal (Fig.7) an additional nonlinearity is introduced when the ICP drops below the given threshold pressure which causes the resistance to absorption to be increased and leads to a lack of absorption until the pressure meets the threshold pressure again [7]. Once that happens absorption again takes place and the system will return to equilibrium.

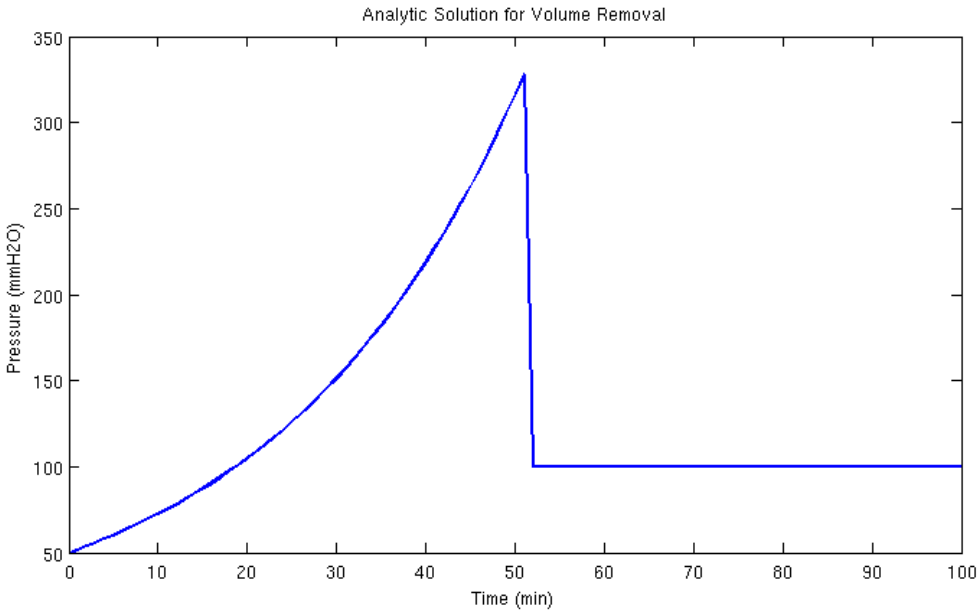

Figure 7: Analytic solution of equation (2.2) for the case of volume removal.

Chapter 3

Stress-Strain Analysis in a Cylindrical Geometry

Consider the two-dimensional problem of elasto-statics, and let

$$\sigma = \begin{pmatrix} \sigma_x & \tau_{xy} & 0 \\ \tau_{xy} & \sigma_y & 0 \\ 0 & 0 & 0 \end{pmatrix}$$

be a plane stress field in a body with the weight force being the only body force acting on the body. Now assume that the body's density is ρ=*constant*. Then the equations of equilibrium are:

$$\begin{cases} \dfrac{\partial}{\partial x}\sigma_x + \dfrac{\partial}{\partial y}\tau_{xy} = 0 \\ \dfrac{\partial}{\partial x}\tau_{xy} + \dfrac{\partial}{\partial y}\sigma_y + \rho g = 0 \end{cases} \tag{3.1}$$

which must be solved for σ_x, σ_y, and τ_{xy} such that they satisfy prescribed boundary conditions. System (3.1) is undetermined because there are only two equations but there are three independent values that need to be determined. In order to get the needed third equation the so-called condition of compatibility of strains will be used which secures the existence of the *u,v*, displacement components. For infinitesimal deformations (linear geometry) the strain components in two dimensions are:

$$\varepsilon_x = \frac{\partial u}{\partial x}, \ \ \varepsilon_y = \frac{\partial v}{\partial y}, \ \ \gamma_{xy} = \frac{\partial u}{\partial y} + \frac{\partial v}{\partial x} \tag{3.2}$$

where *u,v* denote the components of the two dimensional displacement field. It can be shown that the condition of integrability for (3.2) is:

$$\frac{\partial^2 \varepsilon_x}{\partial y^2} + \frac{\partial^2 \varepsilon_y}{\partial x^2} = \frac{\partial^2 \gamma_{xy}}{\partial x \partial y} \tag{3.3}$$

which is called the condition of compatibility for admissible strains.

Now further assume that the body is made of an isotropic linear elastic material, so the inverse of Hooke's Law is:

$$\begin{cases} \varepsilon_x = \dfrac{1}{E}\left(\sigma_x - \nu\sigma_y\right) \\ \varepsilon_y = \dfrac{1}{E}\left(\sigma_y - \nu\sigma_x\right) \\ \gamma_{xy} = \dfrac{2(1+\nu)}{E}\tau_{xy} \end{cases} \tag{3.4}$$

with *E* being the Young's Modulus and *v* the Poisson's ratio. By replacing (3.4) into (3.3) the expression in stresses for the condition of compatibility is:

$$\frac{\partial^2}{\partial y^2}\left(\sigma_x - \nu\sigma_y\right) + \frac{\partial^2}{\partial x^2}\left(\sigma_y - \nu\sigma_x\right) = 2(1+\nu)\frac{\partial^2 \tau_{xy}}{\partial x \partial y} \tag{3.5}$$

By combining the two equations in (3.1) the system is reduced to:

$$\frac{\partial^2 \tau_{xy}}{\partial x \partial y} = -\frac{1}{2}\left(\frac{\partial^2 \sigma_x}{\partial x^2} + \frac{\partial^2 \sigma_y}{\partial y^2}\right)$$

which replaced into (3.5) gives the following Laplace equation:

$$\left(\frac{\partial^2}{\partial x^2}+\frac{\partial^2}{\partial y^2}\right)(\sigma_x+\sigma_y)=0 \tag{3.6}$$

Therefore, (3.1), (3.6) and corresponding boundary conditions can now be solved for the unknown stresses σ_x, σ_y, and τ_{xy}.

In 1862 Airy introduced the so-called Airy stress function $\varphi(x,y)$ such that:

$$\begin{cases}\sigma_x=\dfrac{\partial^2\varphi}{\partial y^2}-\rho g y\\ \sigma_y=\dfrac{\partial^2\varphi}{\partial x^2}-\rho g y\\ \tau_{xy}=-\dfrac{\partial^2\varphi}{\partial x\partial y}\end{cases} \tag{3.7}$$

which when replaced into (3.6) gives the Airy equation for φ:

$$\frac{\partial^4\varphi}{\partial x^4}+2\frac{\partial^4\varphi}{\partial x^2\partial x^2}+\frac{\partial^4\varphi}{\partial y^4}=0. \tag{3.8}$$

The solution to (3.8) and the re-written boundary conditions for φ will then give σ_x, σ_y, and τ_{xy} from (3.7).

Now introducing the polar coordinates:

$$\begin{cases}x=r\cos\theta\\ y=r\sin\theta\end{cases}, \quad \begin{cases}r^2=x^2+y^2\\ \theta=\tan^{-1}\left({}^{y}/_{x}\right)\end{cases}, \quad \begin{cases}\overrightarrow{e_r}=\cos\theta\,\vec{\imath}+\sin\theta\,\vec{\jmath}\\ \overrightarrow{e_\theta}=-\sin\theta\,\vec{\imath}+\cos\theta\,\vec{\jmath}\end{cases}$$

where $\vec{\imath},\vec{\jmath}$ and $\overrightarrow{e_r},\overrightarrow{e_\theta}$, are respectively the orthonormal tangent systems in Cartesian and polar coordinates, and

$$\begin{cases}\frac{\partial r}{\partial x}=\cos\theta, & \frac{\partial r}{\partial y}=\sin\theta\\ \frac{\partial\theta}{\partial x}=-\frac{\sin\theta}{r}, & \frac{\partial\theta}{\partial y}=\frac{\cos\theta}{r}\end{cases}\text{ which implies that }\begin{cases}\frac{\partial}{\partial x}=\frac{\partial r}{\partial x}\frac{\partial}{\partial r}+\frac{\partial\theta}{\partial x}\frac{\partial}{\partial\theta}=\cos\theta\frac{\partial}{\partial r}-\frac{\sin\theta}{r}\frac{\partial}{\partial\theta}\\ \frac{\partial}{\partial y}=\frac{\partial r}{\partial y}\frac{\partial}{\partial r}+\frac{\partial\theta}{\partial y}\frac{\partial}{\partial\theta}=\sin\theta\frac{\partial}{\partial r}+\frac{\cos\theta}{r}\frac{\partial}{\partial\theta}\end{cases}$$

Thus system (3.1) in the absence of any body forces become in polar coordinates:

$$\begin{cases}\frac{\partial\sigma_r}{\partial r}+\frac{1}{r}\frac{\partial\tau_{r\theta}}{\partial\theta}+\frac{\sigma_r-\tau_{r\theta}}{r}=0\\ \frac{1}{r}\frac{\partial\sigma_\theta}{\partial\theta}+\frac{\partial\tau_{r\theta}}{\partial r}+\frac{2\tau_{r\theta}}{r}=0\end{cases}\tag{3.9}$$

while equations (3.7) and (3.8) become:

$$\begin{cases}\sigma_r=\frac{1}{r}\frac{\partial\varphi}{\partial r}+\frac{1}{r^2}\frac{\partial^2\varphi}{\partial\theta^2}\\ \sigma_\theta=\frac{\partial^2\varphi}{\partial r^2}\\ \tau_{r\theta}=-\frac{\partial}{\partial r}\left(\frac{1}{r}\frac{\partial\varphi}{\partial\theta}\right)\end{cases}\tag{3.10}$$

and respectively:

$$\left(\frac{\partial^2}{\partial r^2}+\frac{1}{r}\frac{\partial}{\partial r}+\frac{1}{r^2}\frac{\partial^2}{\partial\theta^2}\right)\left(\frac{\partial^2\varphi}{\partial r^2}+\frac{1}{r}\frac{\partial\varphi}{\partial r}+\frac{1}{r^2}\frac{\partial^2\varphi}{\partial\theta^2}\right)=0\tag{3.11}$$

Now consider an axi-symmetrical stress distribution in a hollow cylinder under uniform pressure on the inner and outer surfaces (Fig.8).

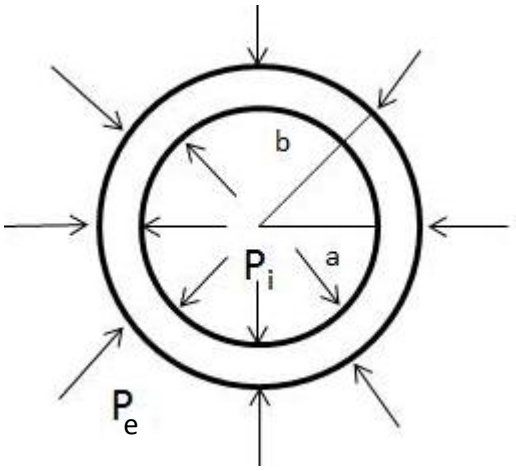

Figure 8: Axi-symmetrical stress distribution in a hollow cylinder under uniform presser on the inner and outer surfaces.

Due to the symmetry of the problem σ_r, σ_θ,$\tau_{r\theta}$, φ are functions of *r* only. The boundary conditions are:

$$\begin{cases}\sigma_r(a) = -P_i(t) \\ \sigma_r(b) = -P_e(t)\end{cases} \qquad (3.12)$$

In this case equation (3.11) reduces to:

$$\frac{d^4\varphi}{dr^4} + \frac{2}{r}\frac{d^3\varphi}{dr^3} - \frac{1}{r^2}\frac{d^2\varphi}{dr^2} + \frac{1}{r^3}\frac{d\varphi}{dr} = 0$$

The solution to the above equation is obtained as follows. Let $\psi = \frac{d\varphi}{dr}$ such that

$$\psi''' + \frac{2}{r}\psi'' - \frac{1}{r^2}\psi' + \frac{1}{r^3}\psi = 0$$

and seek a solution of the form $\psi(r) = r^\alpha$. By replacing this solution in the above differential equation the following characteristic equation is obtained:

$$\alpha(\alpha-1)(\alpha-2) + 2(\alpha-1)\alpha - \alpha + 1 = 0$$

or equivalently:

$$(\alpha-1)[\alpha^2-1] = 0 \rightarrow (\alpha-1)^2(\alpha+1) = 0$$

Thus $\psi(r) = ar + br\ln(r) + \frac{c}{r}$ and since $\int r\ln(r)dr = \frac{r^2}{2}\ln(r) - \frac{r^2}{4}$ it follows that:

$$\varphi(r) = A\ln(r) + Br^2\ln(r) + Cr^2 + D$$

Then the stresses are calculated from equations (3.10) as:

$$\begin{cases}\sigma_r = \frac{A}{r^2} + B\big(1 + 2\ln(r)\big) + 2C \\ \sigma_\theta = -\frac{A}{r^2} + B\big(3 + 2\ln(r)\big) + 2C \\ \tau_{r\theta} = 0\end{cases} \qquad (3.10*)$$

It can be shown that *B=0* in order to have single-valued displacements. The boundary conditions (3.12) give values for A and C and thus it is finally obtained that:

$$\begin{cases} \sigma_r = \dfrac{a^2b^2(P_e - P_i)}{b^2 - a^2}\dfrac{1}{r^2} + \dfrac{P_i a^2 - P_e b^2}{b^2 - a^2} \\ \sigma_\theta = -\dfrac{a^2b^2(P_e - P_i)}{b^2 - a^2}\dfrac{1}{r^2} + \dfrac{P_i a^2 - P_e b^2}{b^2 - a^2} \end{cases} \tag{3.13}$$

From (3.13) it follows that $\sigma_r+\sigma_\theta=const$, which means that σ_r and σ_θ produce a uniform extension or contraction in the direction of the axis of the cylinder.

The radial displacement is found now from:

$$\varepsilon_\theta = \frac{u}{r} = \frac{1}{E}(\sigma_\theta - \nu\sigma_r)$$

since in the two-dimensional case, the strain tensor in polar coordinates is related to the displacement field *(u,v,0)* as follows:

$$\begin{cases} \varepsilon_r = \dfrac{\partial u}{\partial r} \\ \varepsilon_\theta = \dfrac{u}{r} + \dfrac{1}{r}\dfrac{\partial v}{\partial \theta} \\ \gamma_{r\theta} = \dfrac{1}{r}\dfrac{\partial u}{\partial \theta} + \dfrac{\partial v}{\partial r} - \dfrac{v}{r} \end{cases} \tag{3.14}$$

Replacing now formulas (3.10*) into the inverse form of Hooke's Law:

$$\begin{cases} \varepsilon_r = \dfrac{1}{E}(\sigma_r - \nu\sigma_\theta) \\ \varepsilon_\theta = \dfrac{1}{E}(\sigma_\theta - \nu\sigma_r) \\ \gamma_{r\theta} = \dfrac{1}{G}\tau_{r\theta} \end{cases} \tag{3.15}$$

where $G = \frac{E}{2(1+\nu)}$ is the modulus of rigidity (or elasticity in shear), the axi-symmetrical cylinder problem becomes $\gamma_{r\theta} = 0$, and

$$\frac{\partial u}{\partial r} = \frac{1}{E}\left[\frac{(1+\nu)}{r^2}A + 2(1-\nu)B\ln(r) + (1-3\nu)B + 2(1-\nu)C\right]$$

which means that:

$$u(r,\theta) = \frac{1}{E}\left[-\frac{(1+\nu)}{r}A + 2(1-\nu)Br\ln(r) - B(1+\nu)r + 2C(1-\nu)r\right] + f(\theta)$$

and

$$\frac{\partial v}{\partial \theta} = \frac{4Br}{E} - f(\theta)$$

Thus:

$$v(r,\theta) = \frac{4Br\theta}{E} - \int f(\theta)d\theta + g(r)$$

By replacing now *u* and *v* into $\gamma_{r\theta} = 0$ we get:

$$\frac{1}{r}\frac{df(\theta)}{d\theta} + \frac{dg(r)}{dr} + \frac{1}{r}\int f(\theta)d\theta - \frac{1}{r}g(r) = 0$$

This means that $g(r) = Fr$ and $f(\theta) = H\sin\theta + K\cos\theta$.

Therefore:

$$\begin{cases} u(r,\theta) = \frac{1}{E}\left[-\frac{(1+\nu)}{r}A + 2(1-\nu)Br\ln(r) - B(1+\nu)r + 2C(1-\nu)r\right] + H\sin\theta + K\cos\theta \\ v(r,\theta) = \frac{4Br\theta}{E} + Fr + H\cos\theta + K\sin\theta \end{cases}$$

with *A, B, C, F, H, K* constants.

However the term $\frac{4Br\theta}{E}$ in the expression of *v* is multivalued, *i.e.* it changes by 2π as the function goes around the circle once; this implies that $B=0$, since the displacement field must be single valued.

By imposing the boundary conditions (3.12), it can be shown that:

$$\varepsilon_\theta = \frac{1}{E}\left(-\frac{a^2b^2(P_e-P_i)}{b^2-a^2}\frac{1}{r^2}+\frac{P_ia^2-P_eb^2}{b^2-a^2}-\nu\frac{a^2b^2(P_e-P_i)}{b^2-a^2}\frac{1}{r^2}-\nu\frac{P_ia^2-P_eb^2}{b^2-a^2}\right)$$

$$= \frac{1}{E}(-1-\nu)\frac{a^2b^2}{b^2-a^2}(P_e-P_i)\frac{1}{r^2}+\frac{1}{E}(1-\nu)\frac{P_ia^2-P_eb^2}{b^2-a^2}$$

But from equation (3.14):

$$\varepsilon_\theta = \frac{u}{r}+\frac{1}{r}\frac{\partial v}{\partial \theta}$$

and since the problem is axi-symmetric with all the involved function dependent on *r* only, it follows that:

$$u(r) = \frac{1}{E}(-1-\nu)\frac{a^2b^2}{b^2-a^2}(P_e-P_i)\frac{1}{r}+\frac{1}{E}(1-\nu)\frac{P_ia^2-P_eb^2}{b^2-a^2}r \qquad (3.16)$$

The above calculations are intended to be used in the numerical simulations of brain's mechanics. Therefore it is assumed that the brain tissue is made of a homogeneous, isotropic linear elastic solid which fills a hollow cylinder (Fig. 8). It is further assumed that P_i is the effective CSF pressure and P_e is the external boundary pressure due to the presence of the skull. Since the intraventricular CSF volume is almost 1.6% of the total brain volume [8], for a cylindrical geometry it follows that $b\sim 8a$. As in [8] where *Hakim et al.* investigated a similar problem in the spherical geometry, where they say that the case $b>8a$ corresponds to abnormally

small or slit ventricles, while the case $b<8a$ corresponds to dilated ventricles (hydrocephalus). When $b\sim a$ the model represents fully developed hydrocephalus.

Now coupling the mechanics of the brain tissue and the CSF dynamics by assuming that $P_i(t)$, the effective CSF pressure in the ventricles, is given by the Marmarou's model, *i.e.* is the solution to equation (2.2). In order to make this coupling relevant to clinical applications and address some issues related to Marmarou's model, the following medical facts need to be considered:

1) The ventricular wall is made of endotherial cells which are different from brain's cells (neurons and glia cells) and thus the mechano-chemistry of the ventricular wall is different than the one of the brain tissue.
2) The ventricular wall is stiffer than the brain tissue (Mark Iantosca, pediatric neurosurgeon at Hershey Medical Center, private communication).

Thus in the cylindrical model it is assumed that the ventricular wall is a very thin membrane that separates the ventricles filled with CSF and the brain tissue. For the beginning, this membrane will be part of the brain tissue but with different mechanical parameters. More precisely, the Young's modulus of the ventricular wall is bigger than the Young's modulus of the brain tissue. However, during the evolution of hydrocephalus, as the CSF is accumulating in the ventricles, the ventricular wall deforms and becomes stiffer until it gets damaged.

Chapter 4

Results

In this chapter the plots of the displacement given by formula (3.16) for the three cases described in chapter 2 (bolus injection, volume removal and continuous infusion) will be presented. The parameters used in the numerical simulations are given in Table 2.

Table 2: Value of the physical parameters used in simulations.

Parmeter	Value	units
P_e	0	[mmH_2O]
V	.3	[mL]
K	1/.4343	[1/mL]
E	1427.58	[mmH_2O]
v	.35	[-]
a	4.51	[mm]
b	8a	[mm]
r	On plots	[mm]
p_i	From Marmarou's model	[mmH_2O]

P_e is the external boundary condition which is due to the presence of the skull. The MATLAB code used to generate all these plots is provided in Appendix B. There were three values of r plotted on each graph : $r=a$, $r=b$, and respectively $r=(a+b)/2$.

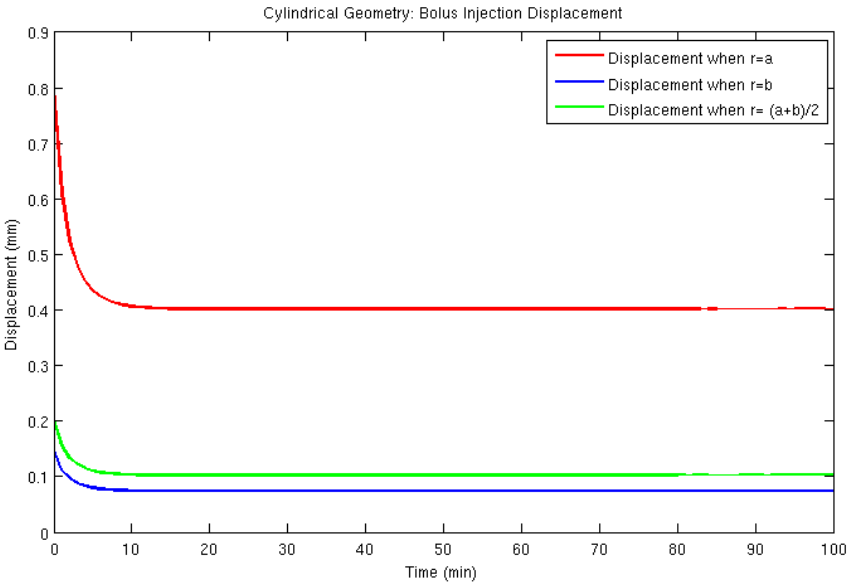

Figure 9: Bolus injection simulation for the displacement.

Fig. 9 corresponds to the bolus injection case with the pressure shown in Fig.5. Notice that both the pressure and the displacement have similar trends. Fig.10 shows the displacement fields in the case of volume removal where the pressue is given in Fig.7, while Fig.11 shows the corresponding displacement fields in the case of continuous infusion whose pressure is shown in Fig.6. As expected, the displacements and pressure fields have the same shapes.

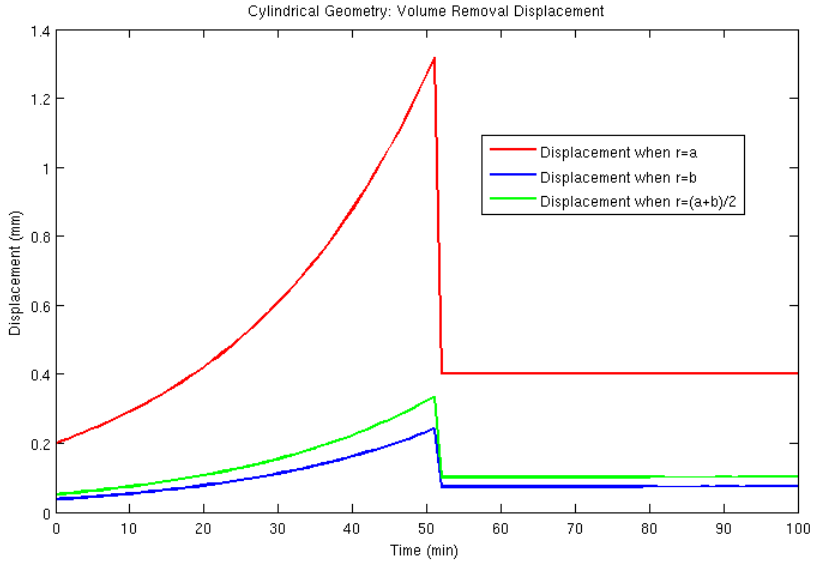

Figure 10: Volume removal simulation for the displacement.

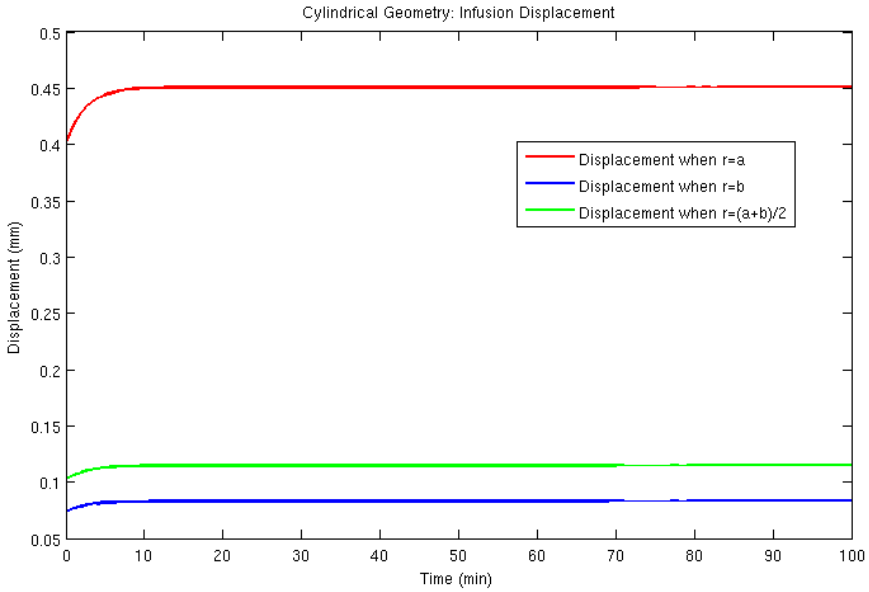

Figure 11: Continuous infusion simulation for the displacement.

Chapter 5

Conclusions and Further Work

In this thesis the mechanics of the brain and of hydrocephalus have been investigated through numerical simulations using two classic mathematical models for the brain: Hakim [8] and Marmarou [7]. The concepts of continuum mechanics and plane elasto-statics have been used to calculate the displacement field in a hollow cylinder made of an isotropic homogeneous linear elastic solid with pressure fields prescribed on the boundaries. The pressure on the interior boundary is given by the solution to Marmarou's model. It has been shown that in the three cases considered in [7]: bolus injection, volume removal, and continuous infusion, the displacement fileds matched the prescribed interior pressure fields. This model is novel in the sense that it uses a cylindrical geometry (rather than the spherical one used in [8]) and a different coupling approach of the brain tissue and the CSF dynamics given by *Marmarou et al.* in [7].

In the proposition of future work on this project it would be suitable to reproduce the experimental settings proposed in [2] (see Figs. 3-4) using some of the novel biomaterials available today. In addition, testing the performance of exiting shunts used by neurosurgeons to treat hydrocephalus, by inserting them in these brain-like phantoms would help to better understand the role of that shunts play in treating hydrocephalus. This controlled environment is essential in increasing the overall understanding of the fundamental science behind brain mechanics and the onset of hydrocephalus. These experiments will be used further to validate the model just proposed in this thesis.

Appendix A

Solutions to Analytic Equation

Here the analytic solutions for bolus injection, volume removal, and continuous infusion from *Marmarou et al*. will be shown.

Bolus Injection

$$I(\tau) = I_f + V\delta(\tau)$$

So then from equation (2.2):

$$\psi_{BI}(t) = e^{K\int_0^t [I_f + V\delta(\tau)]d\tau} = e^{K(I_f t + V)}$$

Also, denote $\gamma_{BI} = \int_0^t \psi_{BI}(\tau)d\tau$ therefore γ_{BI} is:

$$\gamma_{BI}(t) = \int_0^t e^{KI_f\tau + KV} d\tau = \frac{e^{KV}}{KI_f}[e^{KI_f t} - 1]$$

So now

$$P_{BI}(t) = \frac{e^{KI_f t}\left(P_o e^{KV} RI_f\right)}{RI_f + P_o e^{KV}[e^{KI_f t} - 1]}$$

Now note that $I_f = \frac{P_o}{R}$ then

$$P_{BI}(t) = \frac{P_o e^{KV + Kt\frac{P_o}{R}}}{1 + e^{KV}\left[e^{Kt\frac{P_o}{R}} - 1\right]}$$

which agrees with what was given in *Marmarou et al*.

Volume Removal

$$I(\tau) = I_f - V\delta(\tau)$$

Doing the same procedure as above so that:

$$\psi_{VR}(t) = e^{KI_f t - KV}$$

Now denote $\eta_{VR}(t) = \int_0^t \psi_{VR}(\tau)d\tau$ therefore

$$\eta_{VR}(t) = \frac{e^{-KV}}{KI_f}[e^{KI_f t} - 1]$$

Now here there are two cases:

1. The first case is when the resistance is increased because the intracranial pressure is below the threshold pressure. So there is no absorption, so basically $R \rightarrow \infty$.
   So from equation (2.2) since $R \rightarrow \infty$ *P(t)* becomes
   $$P_{VR}(t) = P_o\psi(t) = P_0 e^{K[I_f t - V]}$$
   when the intracranial pressure is below the threshold pressure.

2. The other case is when the intracranial pressure is above the threshold pressure, so getting the equation *P(t)* is found the same as above so therefore *P(t)* is:
   $$P_{VR}(t) = \frac{P_o e^{Kt\frac{P_o}{R} - KV}}{1 + e^{-KV}\left[e^{Kt\frac{P_o}{R}} - 1\right]}$$

Both cases agree with *Marmarou et al*.

<u>Continuous Infusion</u>

$$I(\tau) = I_f + \Delta I$$

Therefore

$$\psi(t) = e^{K\int_0^t (I_f + \Delta I)d\tau} = e^{K(I_f + \Delta I)t}$$

Now denote the integral of ψ as ξ_{CI} so that:

$$\xi_{CI} = \frac{1}{K(I_f + \Delta I)} e^{K(I_f + \Delta I)t} - \frac{1}{K(I_f + \Delta I)}$$

Therefore *P(t)* becomes:

$$P_{CI}(t) = \frac{P_0(P_o + R\Delta I)}{P_o + R\Delta I e^{-Kt\frac{(P_o + R\Delta I)}{R}}}$$

Which again agrees with *Marmarou et al*.

Appendix B

MATLAB Code

Bolus Injection

```
clear all;clc

K=1/0.4343; % units of 1/mL, constant
R=609; % average resistance to CSF absorption calculated from Marmarou
       % paper units of mmH20/mL/min
V=.3;  % Volume of fluid units of mL
Po=100; % units of mmH2O, normal opening (starting pressure level)

t=0:1:100; %t, time measured in minutes

%The solution how Marmarou presents it in the paper
P=(Po*exp(K*V+K.*t.*(Po/R))./(1+exp(K*V).*(exp(K.*t.*(Po/R))-1));

plot(t,P, 'b');

a = 4.15; % mm; radius of the ventricular wall calculated from
          % 4*pi/3*a^3=0.3*10^3 mm^3
          % 1mL=10^3 mm^3
b = 8*a; %mm; radius of the entire cylindrical brain
E=1427.58; % Young's modulus units in mmH2O converted from 14kPa
nu=.35; % Poisson's ratio dimensionless
Pe=0; % external boundary condition due to the presence of the skull

% Plot of Cylindrical Geometry modeling Bolus Injection Method
ua=(1/E)*(-1-nu)*((a.^2*b.^2)/(b.^2-a.^2)).*(Pe-P)*(1/a)+...
    (1/E)*(1-nu).*((a.^2.*P-b.^2*Pe)/(b.^2-a.^2))*a;

figure, plot(t, ua, 'r');

ub=(1/E)*(-1-nu)*((a.^2*b.^2)/(b.^2-a.^2)).*(Pe-P)*(1/b)+...
    (1/E)*(1-nu).*((a.^2.*P-b.^2*Pe)/(b.^2-a.^2))*b;

hold on, plot(t, ub, 'b');

r = (a+b)/2;
ur =(1/E)*(-1-nu)*((a.^2*b.^2)/(b.^2-a.^2)).*(Pe-P)*(1/r)+...
    (1/E)*(1-nu).*((a.^2.*P-b.^2*Pe)/(b.^2-a.^2))*r;

hold on, plot(t, ur, 'g')

xlabel('Time (min)');
ylabel('Displacement (mm)');
title('Cylindrical Geometry: Bolus Injection Displacement');
```

Volume Removal

```
Clear all;clc

K=1/0.4343; % units of mL, constant
R=609; % average resistance to CSF absorption calculated from Marmarou
       % paper units of mmH20/mL/min
V=.3;  % Volume of fluid units of mL
Po=100; % units of mmH2O, normal opening (starting pressure level)
I=.016; % average rate of CSF formation
R1=0; % Reference
Pt=340; % Pressure threshold units of mmH2O from CSF dynamics (Czosnyka)
count=0;
P1=0; %The Presure when it is below the threshold
P2=0; %The Pressure when it is above the threshold
A=[]; %Matrix to get the Pressure out of the for loop
Index=1; % counter to keep track of entries in A

for t=0:1:100 %t, time measured in minutes

    R1=Po.*exp(K*(I.*t-V)); % determine the pressure to see if it is larger
                            % than the threshold pressure.

    if R1<Pt
        P1=Po.*exp(K*(I.*t-V)); % Pressure when the pressure is below
                                % the threshold Pressure
        A(Index)=[P1];
    else
        % Pressure when the pressure is above threshold pressure
        P2=(Po.*exp(-K*V+K*(Po/R).*t))./(1+exp(-K*V).*(exp(K*(Po/R).*t)-1));
        A(Index)=[P2];
    end;

    Index=Index+1;
end;

t=0:1:100;
plot(t,A, 'b');

a = 4.15; % mm; radius of the ventricular wall calculated from
          % 4*pi/3*a^3=0.3*10^3 mm^3
          % 1mL=10^3 mm^3
b = 8*a; %mm; radius of the entire cylindrical brain
E=1427.58; % Young's modulus units in mmH2O converted from 14kPa
nu=.35; % Poisson's ratio dimensionless
Pe=0; % external boundary condition due to the presence of the skull

% Plot of Cylindrical Geometry modeling Volume Removal Method
ua=(1/E)*(-1-nu)*((a.^2*b.^2)/(b.^2-a.^2)).*(Pe-A)*(1/a)+...
    (1/E)*(1-nu).*((a.^2.*A-b.^2*Pe)/(b.^2-a.^2))*a;

figure, plot(t, ua, 'r');

ub=(1/E)*(-1-nu)*((a.^2*b.^2)/(b.^2-a.^2)).*(Pe-A)*(1/b)+...
    (1/E)*(1-nu).*((a.^2.*A-b.^2*Pe)/(b.^2-a.^2))*b;

hold on, plot(t, ub, 'b');
```

```
r = (a+b)/2;
ur =(1/E)*(-1-nu)*((a.^2*b.^2)/(b.^2-a.^2)).*(Pe-A)*(1/r)+...
    (1/E)*(1-nu).*((a.^2.*A-b.^2*Pe)/(b.^2-a.^2))*r;

hold on, plot(t, ur, 'g')

xlabel('Time (min)');
ylabel('Displacement (mm)');
title('Cylindrical Geometry: Volume Removal Displacement');
```

Continuous Infusion

```
Clear all;clc

K=1/0.4343; % units of 1/mL, constant
R=609; % average resistance to CSF absorption calculated from Marmarou
       % paper units of mmH20/mL/min
V=.3;  % Volume of fluid units of mL
Po=100; % units of mmH2O, normal opening (starting pressure level)
delI=.02; % change in I described in Marmarou

t=0:1:100; %t, time measured in minutes

%The solution how Marmarou presents it in the paper
P=(Po*(Po+R*delI))./(Po+(R*delI).*exp(-(K/R)*(Po+R*delI).*t));

plot(t,P, 'b');

a = 4.15; % mm; radius of the ventricular wall calculated from
          % 4*pi/3*a^3=0.3*10^3 mm^3
          % 1mL=10^3 mm^3
b = 8*a; %mm; radius of the entire cylindrical brain
E=1427.58; % Young's modulus units in mmH2O converted from 14kPa
nu=.35; % Poisson's ratio dimensionless
Pe=0; % external boundary condition due to the presence of the skull

% Plot of Cylindrical Geometry modeling Infusion Method
ua=(1/E)*(-1-nu)*((a.^2*b.^2)/(b.^2-a.^2)).*(Pe-P)*(1/a)+...
    (1/E)*(1-nu).*((a.^2.*P-b.^2*Pe)/(b.^2-a.^2))*a;

figure, plot(t, ua, 'r');

ub=(1/E)*(-1-nu)*((a.^2*b.^2)/(b.^2-a.^2)).*(Pe-P)*(1/b)+...
    (1/E)*(1-nu).*((a.^2.*P-b.^2*Pe)/(b.^2-a.^2))*b;

hold on, plot(t, ub, 'b');

r = (a+b)/2;
ur =(1/E)*(-1-nu)*((a.^2*b.^2)/(b.^2-a.^2)).*(Pe-P)*(1/r)+...
    (1/E)*(1-nu).*((a.^2.*P-b.^2*Pe)/(b.^2-a.^2))*r;

hold on, plot(t, ur, 'g')

xlabel('Time (min)');
ylabel('Displacement (mm)');
title('Cylindrical Geometry: Infusion Displacement');
```

References

1. Brunelle F. (2004): Modern Imaging of Pediatric Hydrocephalus. *Pediatric Hydrocephalus*, pp. 79–94.
2. Ciurea AV, Coman TC, Mircea D. (2004): Postinfectious Hydrocephalus in Children. *Pediatric Hydrocephalus*, pp. 201–218.
3. Tuli S, Alshail E, Drake JM. (1999): Third Ventriculostomy versus Cerebrospinal Fluid Shunt as a First Procedure in Pediatric Hydrocephalus. *Pediatric Neurosurgery*, 30(1):11–15.
4. Di Rocco C, Massimi L, Tamburrini G. (2006): Shunts vs. Endoscopic Third Ventriculostomy in Infants: Are There Different Types and/or Rates of Complications? A Review. *Childs.Nerv.Syst*., 22:1573–1589.
5. Hellwig D, Grotenhuis JA, Tirakotai W, Riegel T, Schulte DM, Bauer BL, Bertalanffy H (2005):. Endoscopic Third Ventriculostomy for Obstructive Hydrocephalus. *Neurosurg.Rev.*, 28:1–34.
6. West JJ. (2004): Application of the Level Set Method to Hydrocephalus: Simulating the Motion of the Ventricles. Master's thesis, University of Waterloo.
7. Marmarou, A., Shulman, K., & Rosende, R. M. (1978). A nonlinear analysis of the cerebrospinal fluid system and intracranial pressure dynamics. *Surgical Neurology, 48*, 332-344.
8. Hakim, S., Venegas, J. G., & Burton, J. D. (1976). The physics of the cranial cavity, hydrocephalus and normal pressure hydrocephalus: Mechanical interpretation and mathematical model. *Surgical Neurology, 5*, 187-210.
9. Czosnyka, M., Czosnyka, Z., Momjian, S., & Pickard, J. D. (2004). Cerebrospinal fluid dynamics. *Physiological Measurement, 25*(5).

10. Weerakkody, R. A., Czosnyka, M., Schuhmann, M. U., Schmidt, E., Keong, N., Santarius, T., et al. (2011). Clinical assessment of cerebrospinal fluid dynamics in hydrocephalus. guid to interpretation based on observational study. *Acta Neurologica Scandinavica, 124*, 85-98.

VITA of Justin A. Kauffman

Justin Kauffman
1135 W. Washington St.
Hagerstown, MD 21740
jak5378@psu.edu

EDUCATION **Graduation:** Spring 2012

The Pennsylvania State University, University Park, PA:

Majors: Engineering Science, Honors Curriculum, Bachelors of Science
Mathematics (General Option), Bachelors of Science

Minors: Physics
Nanotechnology
Engineering Mechanics

EXPERIENCE

The Pennsylvania State University Creamery, University Park, PA September 2010 – Current

- Work as student supervisor making sure the shift runs smoothly and provide a good experience for customers.

The Pennsylvania State University Academic Support Center, Mont Alto, PA: February 2009 – May 2010

- Provided peer tutoring and supplementary instruction for various courses including math, chemistry, physics, and computer science.
- Received level 2 certification from the College Reading and Learning Association (CRLA).

The Golden M Company, McDonalds, Hagerstown, MD: June 2006 – July 2010

- Worked as a swing manager and delivered good and fast customer service while maintaining a clean and well run store.

The Pennsylvania State University Honors Research:

- Honors Undergraduate Thesis:
  - Researching Hydrocephalus through Mathematical Modeling and Technological Advancements through computer simulations in MATLAB.
- Bio-diesel project:
  - Researched and developed the bio-diesel project which converted waste vegetable oil from the on campus dining facility into usable bio-fuels.
  - Entered in spring 2009 Academic Festival.
- Dielectric Study:
  - Compared different dielectrics strengths in home-made capacitors
- Physics of Music:
  - Experimentally collected musical waveforms and analyzed frequency data to determine properties of instruments.
  - Entered in spring 2010 Academic Festival.

CLUBS AND ORGANIZATIONS

Society of Engineering Science (SES) Engineering Orientation Network (EON)